Video Article

Fine-tuning the Size and Minimizing the Noise of Solid-state Nanopores

Eric Beamish[1], Harold Kwok[1], Vincent Tabard-Cossa[1], Michel Godin[1,2]

[1]Department of Physics, University of Ottawa

[2]Ottawa-Carleton Institute of Biomedical Engineering, University of Ottawa

Correspondence to: Michel Godin at michel.godin@uottawa.ca

Abstract

Solid-state nanopores have emerged as a versatile tool for the characterization of single biomolecules such as nucleic acids and proteins[1]. However, the creation of a nanopore in a thin insulating membrane remains challenging. Fabrication methods involving specialized focused electron beam systems can produce well-defined nanopores, but yield of reliable and low-noise nanopores in commercially available membranes remains low[2,3] and size control is nontrivial[4,5]. Here, the application of high electric fields to fine-tune the size of the nanopore while ensuring optimal low-noise performance is demonstrated. These short pulses of high electric field are used to produce a pristine electrical signal and allow for enlarging of nanopores with subnanometer precision upon prolonged exposure. This method is performed *in situ* in an aqueous environment using standard laboratory equipment, improving the yield and reproducibility of solid-state nanopore fabrication.

Video Link

The video component of this article can be found at http://www.jove.com/video/51081/

Introduction

Biological and solid-state nanopores provide a means of sensing biomolecular analytes at the single molecule level[1]. Individual nanopores are typically embedded in thin insulating membranes, providing the only conduit for ionic current to pass between two liquid reservoirs. Utilizing the principles of larger-scale Coulter counters, nanopore experiments relate changes in ionic current to determine the length, size, charge and conformation of charged biomolecules as they are electrophoretically driven through a nanopore in the presence of an external electric field.

While biological nanopores such as α-hemolysin typically offer greater sensitivity and low-noise properties[3], the supporting lipid bilayer is fragile and of fixed size, limiting their applicability. Solid-state nanopores, on the other hand, are fabricated in thin (10-50 nm) silicon nitride or silicon oxide membranes and can be made of different sizes, be readily integrated with wafer-scale technologies[6,7], and are more robust, allowing for a wider range of experimental conditions. Despite these advantages, solid-state nanopore technologies suffer from several practical drawbacks that limit their usefulness for biomolecular studies. While control of nanopore size is possible, it is typically expensive and laborious to achieve, requiring specialized equipment and skilled personnel. For example, nanopores drilled by focused-ion beam have been recently shown to shrink under specific experimental conditions in a scanning electron microscope (SEM)[5]. In other approaches, nanopores drilled by transmission electron microscopy (TEM) can expand or shrink depending on the beam conditions and subsequent exposure to aqueous solvents[8]. In these cases, the achievable range of nanopore sizes is limited, difficult to control and even unreliable as the size of the nanopore can change following chemical treatment or when immersed in a particular liquid environment[9].

The ionic current through solid-state nanopores can also suffer from high noise, the sources of which are an intensely investigated topic in nanopore literature[2,3,10,11]. While various methods have been proposed to reduce electrical noise, the yield of reliable, stable low-noise nanopores is typically low. Deposition of carbonaceous residues during drilling and imaging can have detrimental effects on the electrical signal quality, often making complete wetting a challenge and causing the formation of nanobubbles that can be difficult to remove[12]. Furthermore, clogging of the nanopore by analyte molecules degrades signal quality rendering pores unusable for further experiment[13,14]. Altogether, these effects greatly reduce yield of functional nanopore devices and increase the cost associated with solid-state nanopore research.

The application of a voltage with Ag/AgCl electrodes to produce high electric fields in the range of 0.15-0.3 V/nm presents a surprisingly simple solution to these challenges. Through the cyclic application of short voltage pulses, a clean, low-noise nanopore surface ideal for single-molecule studies is produced. Prolonged exposure to high electric fields initiates the removal of the membrane material constituting the pore wall, resulting in an increase in nanopore diameter. This growth can be precisely controlled by tuning the pulse strength and duration. As current traces degrade over the course of an experiment due to clogging of the nanopore as molecules adsorb to the nanopore surface, this process can be repeated to recover clogged devices that would have otherwise been discarded. As such, the yield of functional nanopores is further

increased by the ability to use the same device multiple times. This method provides several advantages as it is rapidly performed in liquid under experimental conditions, requires only standard laboratory equipment, can be automated with software, and produces functional high-quality nanopores with a yield of over 95%.

Protocol

1. Nanopore Fabrication and Cleaning

Note: Once a nanopore exists in an insulating membrane, it can be directly mounted in the liquid cell without further processing or cleaning, as described in step 2. However, if it is necessary to remove traces of contaminants between experiments, nanopore chips can be cleaned using either piranha solution[3,15,16] (3:1 H_2SO_4:H_2O_2) or by exposure to oxygen plasma[2]. As such, steps 1.2 to 1.9 in the following protocol are optional if precleaning by exposure to piranha solution is not necessary.

1. Degas filtered deionized (DI) water by placing under vacuum in a sonicator for 30 min at 40 °C.
2. Prepare piranha solution in a 10 ml beaker by carefully adding 3 ml sulfuric acid followed by 1 ml hydrogen peroxide. Mix thoroughly by refluxing in the pipette. CAUTION: Piranha solution is extremely hazardous. Please take all precautions.
3. Using acid-resistant tweezers, carefully insert the nanopore-containing membrane chip edge-first into the piranha solution to completely submerge the chip and avoid it floating on the surface.
4. Rinse tweezers thoroughly in filtered water.
5. Place the beaker on a hot-plate preset to 90 °C and allow it to clean for at least 30 min.
6. Carefully remove the piranha solution from the beaker using a clean glass pipette and discard in copious amounts of water.
7. Using a clean glass pipette add 5 ml of the degassed deionized water from step 1.1 into the beaker to rinse. Remove the water and repeat at least 5x.
8. Carefully remove the nanopore chip from the beaker using clean sharp-tip tweezers. Handle with extreme care as the nanopore membrane is very fragile.
9. Dry the chip by gently applying suction to its edge using an aspirator. Store the chip in a clean Petri dish until ready for use.

2. Mounting the Nanopore

1. Clean the Teflon nanopore cell (**Figure 1**) by placing in 20% nitric acid solution and boiling for 10 minutes. CAUTION: Use all necessary personal protective equipment and handle acids with care.
2. Carefully remove the cell from nitric acid and place in boiling DI water for 10 min.
3. Boil the cell in DI water for an additional 10 min to ensure complete removal of nitric acid. Remove the beaker from the hot plate and allow it to cool to room temperature.
4. Remove the cell from the beaker and blow dry with filtered air or N_2. Store the cell in a clean Petri dish.
5. Degas filtered KCl solution (buffered with HEPES at pH 8) by placing under vacuum in a sonicator for 30 min at 40 °C.
6. Clean two silicone elastomer gaskets for each nanopore chip by sonicating in ethanol for at least 10 min.
7. Place the nanopore chip on a clean elastomer gasket being careful to align the membrane window with the gasket opening. Place and align a second gasket atop the chip.
8. Place the chip and gaskets on the reservoir inlet of one half of the cleaned nanopore cell. Assemble the cell by screwing the other half in place. An exploded view of the nanopore cell components is shown in **Figure 1.**
9. Wet the nanopore chip by pipetting ethanol into the cell reservoirs and placing in a vacuum chamber until a few bubbles are seen to exit the inlets.
10. Remove ethanol by flushing the reservoirs with at least 3 ml degassed filtered KCl solution. Take care to remove overflow using an aspirator.

3. Nanopore Characterization

1. Place the nanopore cell in the electrically shielded experimental setup and place Ag/AgCl electrodes in each reservoir. This setup is similar to that shown in **Figure 2** with the exception of the external power supply and current amplifier which are replaced with a low-noise resistive feedback amplifier.
2. Using the low-noise amplifier in voltage-clamp mode, apply potentials sweeping from -200 mV to +200 mV and record the I-V characteristics.
3. Fit the I-V curve to obtain nanopore conductance, which can be used to calculate its diameter in solution[17]. If the calculated diameter is much smaller than expected from TEM imaging, the pore is likely not completely wetted and/or contains debris or contamination.
4. Apply a 200 mV potential across the nanopore and record the ionic current for 30 sec.
5. Perform a power spectral density (PSD) analysis of the ionic current and integrate to quantify the electrical noise characteristics of the nanopore. If the noise is above 15 pA RMS at 5 kHz bandwidth, then the pore is likely not completely wetted and/or contains contamination and cannot be reliably used in experiment.

4. Conditioning Nanopores Using High Electric Fields

Note: If the I-V curve generated exhibited asymmetry or less-than-expected conductance, or the current trace showed instability and high noise levels at low-frequencies, it is necessary to condition the nanopore with high electric fields to remove any contamination on the pore surface and/or wet the pore. While this method does not affect the high-frequency noise caused by the membrane capacitance or any parasitic capacitance coupled to the input of the current amplifier used in measurements, low-frequency noise (also called 1/f noise)[18] can be greatly reduced. A schematic of the setup used to perform this conditioning is shown in **Figure 2.**

1. Disconnect the electrodes from the patch-clamp amplifier.
2. Connect one of the electrodes to a computer-controlled power supply capable of generating >6 V (>0.2 V/nm electric field strength for the 30-nm thick membranes used here) and the other to an external current amplifier that can be monitored in real time.
   Note: The application of high electric fields can be used to condition nanopores in various membrane materials and thicknesses. While both 30-nm and 10-nm membranes are discussed here, voltages described refer to those used for 30-nm thick membranes unless otherwise stated.
3. Apply a potential difference of 400 mV (measurement voltage) across the nanopore for at least 5 sec.
4. Calculate the mean current value from the final 1 sec of data to determine the conductance of the nanopore. Calculate the diameter of the nanopore based on this conductance, which should be done automatically using the software and the nanopore conductance model of choice based on the most likely geometry. It should correspond to the diameter measured from the I-V curve.
5. Apply a 200 msec pulse of 6 V (wetting voltage) across the nanopore to produce an electric field of 0.2 V/nm followed by a 5 sec measurement period at 400 mV. Again, calculate a diameter of the nanopore using the final 1 sec of data and compare with the value expected from TEM measurements to ensure that the nanopore is fully wet. If necessary, repeat several times.
6. If necessary, repeat the application of high electric field pulses with increasing voltage until the current signal during the measurement period is stable and showing the expected conductance. It is not recommended to exceed 10 V (*i.e.* >0.3 V/nm), as this can significantly enlarge or damage the nanopore rapidly.

5. Enlarging Nanopores Using High Electric Fields

Note: The diameter of the nanopore is crucial in determining its functionality for a particular biomolecular sensing application. To this end, a nanopore created using a TEM can be enlarged to a desired size by applying high electric fields until the appropriate diameter is achieved with the same setup used to clean and wet the nanopore (**Figure 2**).

1. Using the same electronic configuration as in part 4, apply a 200-500 mV bias across the pore to obtain a diameter measurement. While less precise than fitting an I-V curve, a single point measurement can be used to roughly estimate the nanopore size rapidly.
2. Apply a 2 sec pulse of 8 V across the nanopore followed by a measurement period of at least 5 sec at 400 mV. Calculation of the new diameter will typically show a very small increase in nanopore size (<0.1 nm).
3. Repeat this process cyclically, alternating between enlargement and measurement voltages to obtain *in situ* and real-time measurements of increasing nanopore diameter.
4. If faster growth rate is desirable, increase the magnitude of the voltage applied incrementally up to 10 V. Growth will typically accelerate as the pore enlarges with the rate of increase in conductance ranging from 0.03 nS/sec to 10 nS/sec, depending on the size of the nanopore, strength of the electric field and electrolyte solution properties.
5. When the desired diameter is reached, stop the application of high electric fields. This can be done automatically using the computer program.
6. Reconnect the patch-clamp amplifier to the electrodes.
7. Acquire new I-V and current trace data at 200 mV to confirm the diameter of the nanopore and verify low-noise current signals as in steps 3.2 - 3.5 above. If necessary, repeat conditioning and enlarging protocol (steps 4.1 - 5.5).

6. DNA Translocation

1. Prior to adding a biomolecular sample, perform a control experiment to ensure that there is no contamination in the reservoir. Acquire a current trace under an applied potential of +150 to +300 mV in the absence of any sample to verify that no current blockades are detected after 2 min.
2. Add λ DNA (48.5 kbp double-stranded) to the *cis* reservoir for a final concentration of 0.5-2 ng/μl. Reflux gently by pipette for at least 10 sec to ensure homogeneous distribution of the sample throughout the reservoir.
3. For a 30-nm thick nanopore, apply a potential bias of +150 to +300 mV to the *trans* reservoir and measure the ionic current passing through the nanopore. For very short translocation events, it is desirable to sample at a high frequency (250 kHz or greater) with a relatively high low-pass filtering frequency (100 kHz).
4. Monitor the ionic current using software to detect transient current blockades as molecules translocate through the nanopore. The ionic current traces of molecular translocation can be analyzed to determine blockage depth, duration and frequency to infer information about the sample of interest. Conversely, if information about the translocating molecules is known, this data can be used to investigate properties of the nanopore itself.

Representative Results

The nanopores used in this study were drilled in 30-nm or 10-nm thick silicon nitride membrane windows. While the protocol described can be applied to solid-state nanopores of various material fabricated using any method, they are commonly drilled by TEM using previously established protocols[11,14]. Nanopores drilled by TEM are typically between 4-8 nm in diameter (**Figure 2**). While both 30-nm and 10-nm thick membranes can be mounted and conditioned using the above protocol, voltage biases described refer those required for 30-nm thick membranes unless otherwise stated. For membranes of different size, the applied voltage should be adjusted to generate an electric field in the range of 0.15-0.3 V/nm inside the nanopore.

Figure 3a shows two typical conductance traces of a 10-nm nanopore in a 30-nm thick membrane before and after treatment with high electric fields. Upon mounting a newly drilled nanopore, the likelihood of obtaining an unstable and noisy ionic current signal, exhibiting a high degree of low-frequency fluctuation, is usually high. The nanopore shown in **Figure 3a** highlights this behavior. Its conductance is considerably less than expected for a nanopore of its size, most likely due to incomplete wetting. Upon the application of high electric fields of 0.27 V/nm in magnitude produced by 8 V pulses (90 pulses of 2 sec duration), the nanopore becomes fully wet and is subsequently enlarged to 21 nm in diameter. At this

point, the pore exhibits a stable conductance with low-noise properties. Quantitative analysis of noise in similar nanopores is shown as power spectral density plots in **Figure 3b**. The low-frequency noise amplitude of unwet and/or clogged pores is very high (>20 pA RMS), rendering them unusable in experiment. Upon conditioning with high electric fields, noise power at low frequencies (<10 kHz) is diminished by up to 3 orders of magnitude and ready for low-noise experiments.

Figure 4a shows a typical current measurement as the potential applied is pulsed between high electric fields for enlarging and low electric field measurement periods. After each subsequent pulse, the resultant ionic current through the nanopore at the measurement voltage (*i.e.* the nanopore conductance) increases by a finite amount. This demonstrates that the nanopore is increased in size, as the diameter *d* can be inferred from its conductance *G* in a solution of conductivity σ, approximating the nanopore as having cylindrical geometry of effective length l_{eff}. While various other models exist for relating nanopore conductance to its geometry[17,19-21], the following relation, which incorporates a geometric term and an access resistance term, has been proven valid for TEM-drilled nanopores in high salt concentrations, over a wide range of diameters of interest for dsDNA translocation[17,22].

$$G = \sigma \left[\frac{4l_{eff}}{\pi d^2} + \frac{1}{d} \right]^{-1}$$

Once the desired diameter is reached, the process is automatically stopped by the software. The resulting nanopore diameter can then be confirmed using precise I-V measurements, as shown in **Figure 4b**.

It is important to note that nanopores treated using high electric fields are fully functional. This is validated by the detection of λ DNA translocation, as shown in the conductance traces presented in **Figure 5a**. In this figure, dsDNA is driven through two nanopores that were enlarged to 11-nm and 32-nm using the described method. In each case, the baseline conductance is extremely stable and clear blockades are observed as dsDNA molecules translocate through the nanopore, displaying high signal-to-noise single-molecule translocation events as compared to untreated pores that exhibit high noise. As shown in the insets of **Figure 5a**, multiple discrete blockage levels are observed as individual folded molecules translocate, as expected for nanopores of these sizes. Histograms of the nanopore conductance during translocation events through each pore are shown in **Figure 5b**. The low-noise properties of the nanopores reveal distinct, easily resolvable peaks corresponding to the baseline (no DNA), single (one DNA strand - unfolded) and double blockage states (two DNA strands - folded). Of note is the fact that the change in conductance corresponding to a single dsDNA molecule occupying the pore is different for the large and small nanopores. This provides indirect evidence that the application of high electric fields is in fact enlarging existing nanopores, as the same blockage amplitude would be observed if other pores or cracks were being created in the membrane during the process[17].

Similarly, **Figure 6** illustrates the effectiveness of high electric fields for enlarging nanopores fabricated in membranes of different thickness. Here, a nanopore created in a 10-nm SiNx membrane is initially partially unwet, displaying unstable and relatively small conductance. Upon the application of alternating ±3 V (±0.3 V/nm) pulses of 4 sec duration (30 total), the nanopore becomes wet and exhibits ideal I-V characteristics for a 3 nm pore. The methodology was then repeated for 400 subsequent pulses and the nanopore was enlarged to 8 nm. This enlargement, performed at comparable electric fields but lower applied voltage bias than for nanopores fabricated in 30-nm membranes, shows that the process is primarily electric field driven. As the current blockade produced by translocation through a thinner membrane is larger than that produced in thicker pores, nanopores in thin membranes treated in this fashion can be used to study shorter molecules such as proteins with increased sensitivity.
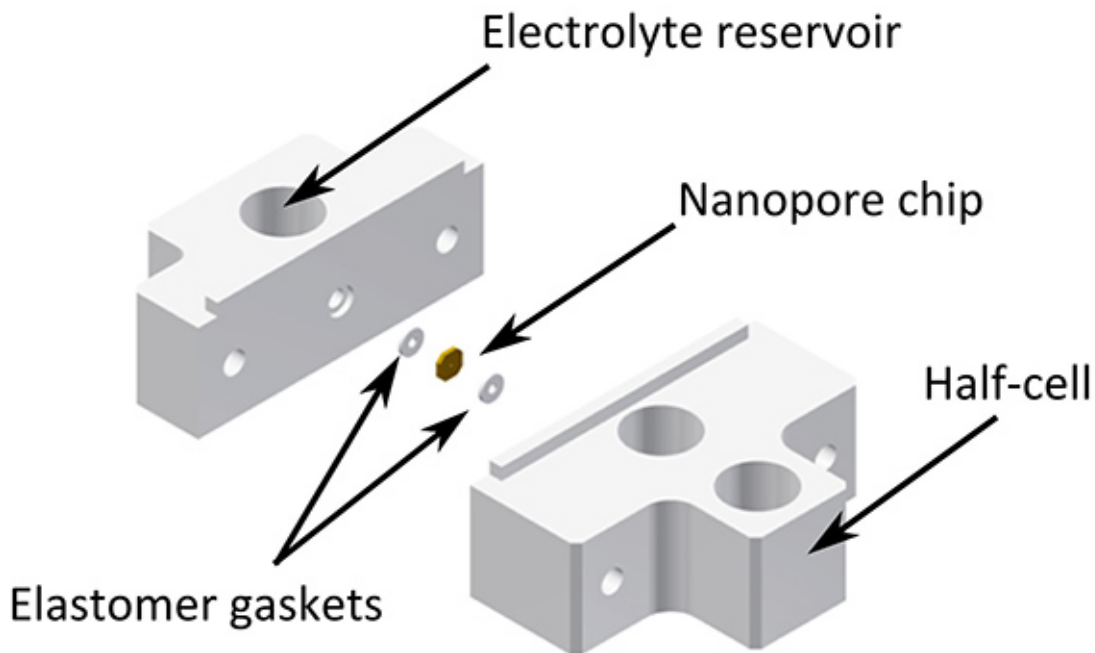
Figure 1. Nanopore cell assembly. A silicon nitride membrane containing a nanopore is placed between silicone elastomer gaskets, which are in turn compressed by two Teflon half-cells containing electrolyte reservoirs. Click here to view larger image.
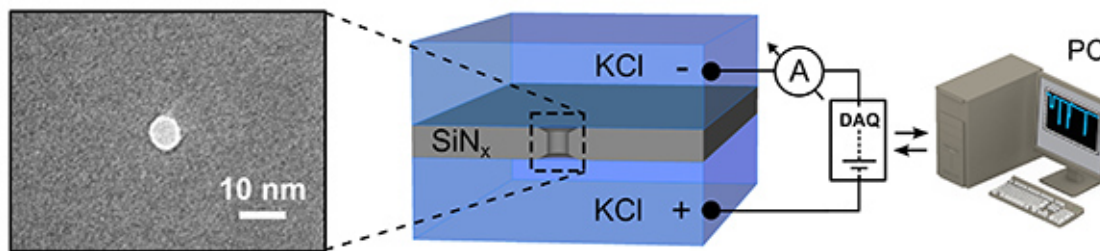

Figure 2. Nanopore conditioning and enlarging setup. A nanopore drilled in a 30 nm thick silicon nitride membrane (left) connects two electrolyte reservoirs. A computer is used to control either a patch-clamp amplifier or external power supply (DAQ card) which applies a potential bias across the nanopore via Ag/AgCl electrodes immersed in the electrolyte reservoirs. The current amplifier relays the ionic current measured to be monitored in real time using computer software. This figure has been modified from [11]. Click here to view larger image.
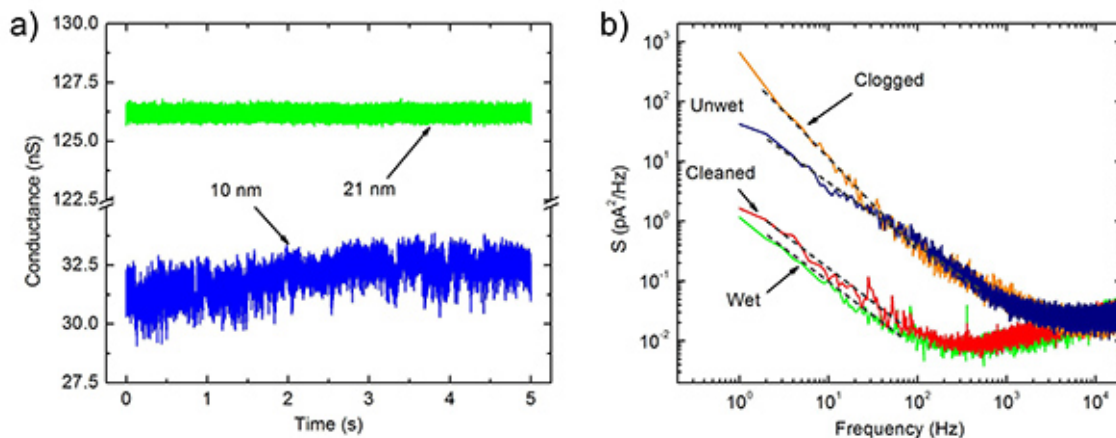
Figure 3. Current traces before and after application of high electric fields. (**a**) Upon mounting, and even following cleaning with piranha solution, the conductance of the nanopore is unstable and less than expected for a cylindrical 10-nm pore (blue). After the application of 2 sec pulses of 8 V, the nanopore is fully wetted and enlarged, exhibiting a stable conductance and can be used for biomolecular sensing experiments (green). (**b**) Power spectral density plots of an incompletely wetted and clogged nanopore (blue and orange, respectively). Upon application of 200 msec pulses of 8 V, the nanopores were wetted and debris removed (green and red, respectively). This figure has been modified from [11]. Click here to view larger image.
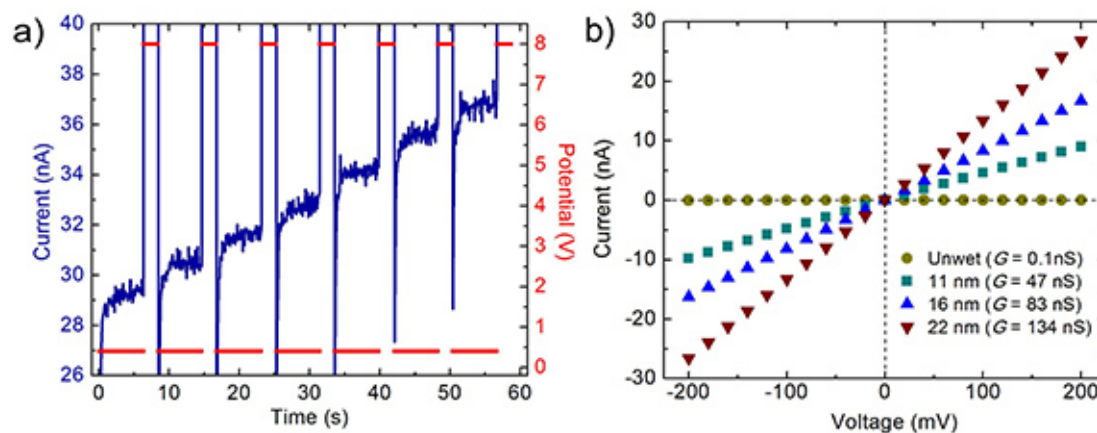
Figure 4. Nanopore enlarging using high electric fields. (**a**) Alternating between enlargement and measurement potential biases (red) reveals that the ionic current through the nanopore (blue) increases in finite steps. The resulting conductance measurement can be used to infer nanopore diameter. Once the desired diameter has been achieved, the process is stopped. (**b**) Precise I-V measurements of conductance confirm that nanopore sizes have increased. Such plots provide a better estimate of the pore size than single-point current values as they can be fit and their symmetric and Ohmic behavior can be confirmed. This figure has been modified from [11]. Click here to view larger image.
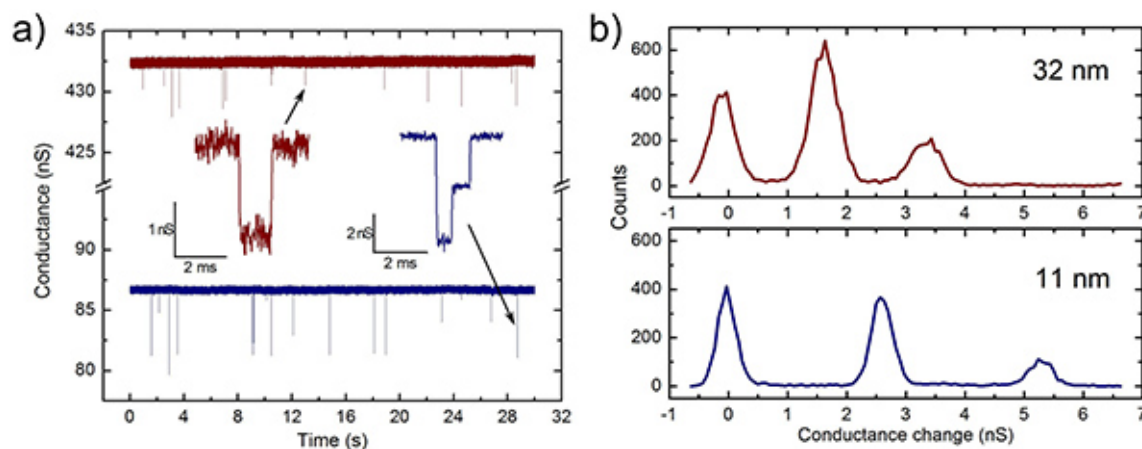
Figure 5. DNA translocation through conditioned nanopores. (a) The addition of dsDNA (48.5 kbp) to one side of the nanopore at a bias of 150 mV produces transient blockades in the conductance traces of 11-nm (blue) and 32-nm pores (red). **(b)** Histograms of the conductance of each of the nanopores show discrete peaks corresponding to the baseline, single and double translocation events. This figure has been modified from [11]. Click here to view larger image.
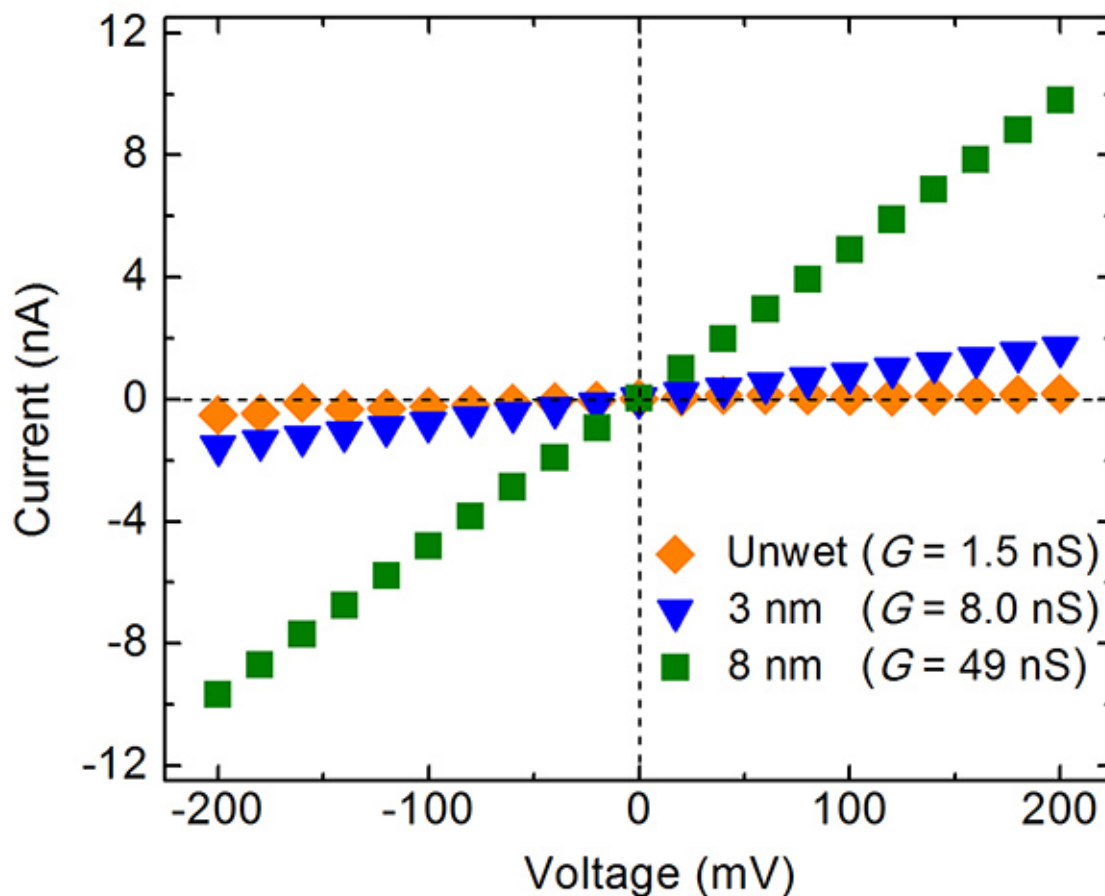
Figure 6. Enlargement of nanopores in 10 nm membranes. A nanopore in a 10 nm membrane originally exhibits very little conductance and asymmetric I-V characteristics (orange). Upon the application of 30 pulses of alternating between ±3 V (4 sec duration), the nanopore wets and exhibits ideal I-V properties with a conductance consistent with that expected for a 3 nm pore (blue). A further 400 pulses of ±3 V enlarges the nanopore to a diameter of 8 nm (green). Click here to view larger image.

Discussion

Control of nanopore size is of fundamental importance in biomolecular sensing applications. Nanopore diameters must be on the order of the size of the molecules being probed; they must be large enough to accommodate the sample but small enough to achieve optimal signal-to-noise. While the control of size using the method presented of applying high electric fields is unidirectional in that nanopore diameters are only *increased* throughout the process, nanopores with diameters between 3-100 nm can be fashioned, with subnanometer precision. As 3-4 nm pores can be readily fabricated using a TEM[23,] this allows for the reliable fabrication of solid-state nanopores for a wide range of applications from probing ssDNA structure to the interaction of bulky protein-ligand complexes. While nanopore growth above 100 nm can be very fast and less precise, more moderate enlarging conditions can be employed to achieve better control over the process. As such, the most important step for achieving effective size control is the choice of pulse strength and duration in order to balance enlarging efficiency and the level of precision required in achieving a desired pore diameter. This is further highlighted by the enlargement of thinner nanopores (10-nm thickness), where enlargement is observed a lower bias but comparable electric field strength. Depending on the final size, it is generally possible to enlarge a nanopore to sub-100-nm diameters in a few minutes.

Similarly, large low-frequency current fluctuations preclude single-molecule studies as it is nearly impossible to differentiate translocation signals from background noise. Incomplete wetting[24], the presence of carbonaceous residues remaining after initial fabrication[25] and adsorption of debris on the nanopore wall[13] can degrade signal quality, requiring additional cleaning with harsh chemical treatments that are often inefficacious. Interestingly, it is common for solid-state nanopore protocols to emphasize the importance of cleaning the nanopore in piranha solution or with oxygen plasma before mounting to aid wetting or remove any contamination left over from the drilling, imaging and handling processes. Even with this treatment, however, nanopores often do not wet or continue to exhibit high noise, and the suggested solution for failed attempts is to perform additional cleaning which can be extremely time consuming[14]. With the application of high electric fields, these lengthy protocols may not be necessary depending on the application. It was found that most devices could be reconditioned *in situ* using the method described herein, consequently reducing preparation time and the need to deal with harsh chemicals. The most important steps in mitigating electrical noise is a simple increase in voltage and/or pulse duration to completely wet the pore and remove loosely-bound debris. Nanopores treated in this fashion can reliably be used in biomolecule translocation experiments, such as the passage of DNA and proteins. If these molecules adhere to the pore wall leading to a clogged and noisy electrical signal, high electric field pulses can be reapplied to remove the obstruction and regain low-noise properties for further experimentation, without unmounting of the nanopore chip from the fluidic cell.

The application of high electric fields using the setup described is limited by the requirement of an external power supply that can apply up to 10 V and current amplifier, which lack the sensitivity and low-noise properties at high-bandwidth (>1 kHz) for single molecule sensing. While typical biomolecular experiments rely on a low-noise current amplifier that is limited to ±1 V, it is straightforward to design a single system that could accomplish both high electric field conditioning and sensitive current measurement with an adjustable gain. Despite this limitation, the transition from one setup to the other is quick and straightforward. In comparison with existing techniques for controlling nanopore size such as the use of SEM[5], thermal oxidation and membrane reshaping[8], high electric fields offer a faster, more precise and less expensive methodology that can be performed on the lab bench using standard equipment and provide a broader range of nanopore sizes. The ability to rapidly and reproducibly reduce low-frequency noise also makes initial fabrication more reliable and prolongs the lifetime of solid-state nanopores, as previously used pores can be rejuvenated for further experiments. Altogether, over 95% of nanopores of varying thicknesses conditioned with high electric fields exhibited very little low-frequency noise characteristic, rendering them suitable for biomolecule sensing. Fabrication is thus easier and more reliable, making solid-state nanopore experiments more accessible to researchers and potentially allowing for a path towards commercialization of nanopore technologies through more robust fabrication processes.

Disclosures

The authors have nothing to disclose.

Acknowledgements

References

1. Venkatesan, B. M. & Bashir, R. Nanopore sensors for nucleic acid analysis. *Nat. Nanotechnol.* **6** (10), 615-624, doi:10.1038/nnano.2011.129 (2011).
2. Smeets, R. M. M., Keyser, U. F., Dekker, N. H. & Dekker, C. Noise in Solid-State Nanopores. *Proc. Natl. Acad. Sci. U.S.A.* **105** (2), 417-421, doi:10.1073/pnas.0705349105 (2008).
3. Tabard-Cossa, V., Trivedi, D., Wiggin, M., Jetha, N. N. & Marziali, A. Noise analysis and reduction in solid-state nanopores. *Nanotechnology.* **18**, 305505 doi:10.1088/0957 4484/18/30/305505 (2007).
4. Wu, M.-Y. *et al.* Control of Shape and Material Composition of Solid-State Nanopores. *Nano Lett.* **9** (1), 479-484, doi:10.1021/nl803613s (2009).
5. Prabhu, A. S., Freedman, K. J., Robertson, J. W. F., Nikolov, Z., Kasianowicz, J. J. & Kim, M. J. SEM-induced shrinking of solid-state nanopores for single molecule detection. *Nanotechnology.* **22**, 425302 doi: 10.1088/0957 4484/22/42/425302 (2011).

6. Li, J., Stein, D., McMullan, C., Branton, D., Aziz, M. J. & Golovchenko, J. A. Ion-beam sculpting at nanometre length scales. *Nature.* **412** (6843), 166-169, doi:10.1038/35084037 (2001).
7. Rosenstein, J. K., Wanunu, M., Merchant, C. A., Drndic, M. & Shepard, K. L. Integrated nanopore sensing platform with sub-microsecond temporal resolution. *Nat. Methods.* **9** (5), 487-492, doi:10.1038/nmeth.1932 (2012).
8. Van den Hout, M., Hall, A. R., Wu, M. Y., Zandbergen, H. W., Dekker, C. & Dekker, N. H. Controlling nanopore size, shape and stability. *Nanotechnology.* **21**, 115304 doi: 10.1088/0957 4484/21/11/115304 (2010).
9. Li, Q. *et al.* Size evolution and surface characterization of solid-state nanopores in different aqueous solutions. *Nanoscale.* **4** (5), 1572-1576, doi:10.1039/C2NR12040B (2012).
10. Smeets, R., Dekker, N. & Dekker, C. Low-frequency noise in solid-state nanopores. *Nanotechnology.* **20**, 095501 doi: 10.1088/0957 4484/20/9/095501 (2009).
11. Beamish, E., Kwok, H., Tabard-Cossa, V. & Godin, M. Precise control of the size and noise of solid-state nanopores using high electric fields. *Nanotechnology.* **23** (40), 405301, doi:10.1088/0957-4484/23/40/405301 (2012).
12. Smeets, R. M. M., Keyser, U. F., Wu, M. Y., Dekker, N. H. & Dekker, C. Nanobubbles in Solid-State Nanopores. *Phys. Rev. Lett.* **97** (8), 088101, doi:10.1103/PhysRevLett.97.088101 (2006).
13. Niedzwiecki, D. J., Grazul, J. & Movileanu, L. Single-Molecule Observation of Protein Adsorption onto an Inorganic Surface. *J. Am. Chem. Soc.* **132** (31), 10816-10822, doi:10.1021/ja1026858 (2010).
14. Niedzwiecki, D. J. & Movileanu, L. Monitoring Protein Adsorption with Solid-state Nanopores. *J. Vis. Exp.* (58), e3560, doi:10.3791/3560 (2011).
15. Wanunu, M & Meller, A. Single-molecule analysis of nucleic acids and DNA-protein interactions. *Single-molecule techniques: a laboratory manual*. Cold Spring Harbor Laboratory Press: New York, 395-420 (2008).
16. Tabard-Cossa, V. Instrumentation for Low-Noise High-Bandwidth Nanopore Recording. *Engineered Nanopores for Bioanalytical Applications*. 59-93 (2013).
17. Kowalczyk, S. W., Grosberg, A. Y., Rabin, Y. & Dekker, C. Modeling the conductance and DNA blockade of solid-state nanopores. *Nanotechnology.* **22** (31), 315101, doi:10.1088/0957-4484/22/31/315101 (2011).
18. Siwy, Z. & Fuliński, A. Origin of 1/fα Noise in Membrane Channel Currents. *Phys. Rev. Lett.* **89** (15), 158101, doi:10.1103/PhysRevLett.89.158101 (2002).
19. Liebes, Y. *et al.* Reconstructing solid state nanopore shape from electrical measurements. *Appl. Phys. Lett.* **97** (22), 223105, doi:10.1063/1.3521411 (2010).
20. Kim, M. J., Wanunu, M., Bell, D. C. & Meller, A. Rapid Fabrication of Uniformly Sized Nanopores and Nanopore Arrays for Parallel DNA Analysis. *Adv. Mater.* **18** (23), 3149-3153, doi:10.1002/adma.200601191 (2006).
21. Smeets, R. M. M., Keyser, U. F., Krapf, D., Wu, M.-Y., Dekker, N. H. & Dekker, C. Salt Dependence of Ion Transport and DNA Translocation through Solid-State Nanopores. *Nano Lett.* **6** (1), 89-95, doi:10.1021/nl052107w (2006).
22. Wanunu, M., Dadosh, T., Ray, V., Jin, J., McReynolds, L. & Drndić, M. Rapid electronic detection of probe-specific microRNAs using thin nanopore sensors. *Nat. Nanotechnol.* **5** (11), 807-814, doi:10.1038/nnano.2010.202 (2010).
23. Dekker, C. Solid-state nanopores. *Nat. Nanotechnol.* **2** (4), 209-215 doi:10.1038/nnano.2007.27 (2007).
24. Powell, M. R., Cleary, L., Davenport, M., Shea, K. J. & Siwy, Z. S. Electric-field-induced wetting and dewetting in single hydrophobic nanopores. *Nat. Nanotechnol.* **6** (12), 798-802, doi:10.1038/nnano.2011.189 (2011).
25. Egerton, R. F., Li, P. & Malac, M. Radiation damage in the TEM and SEM. *Micron.* **35** (6), 399-409, doi:10.1016/j.micron.2004.02.003 (2004).

October 2013 | 80 | e51081 | Page 9 of 9